Front. Electr. Electron. Eng. China 2011, 6(2): 339–346
DOI 10.1007/s11460-011-0151-1

RESEARCH ARTICLE

Xudong ZHAO, Peng LIU, Jiafeng LIU, Xianglong TANG

Feature extraction for classification of different weather conditions

Abstract Classification of different weather conditions provides a first step support for outdoor scene modeling, which is a core component in many different applications of outdoor video analysis and computer vision. Features derived from intrinsic properties of the visual effects of different weather conditions contribute to successful classification. In this paper, features representing both the autocorrelation of pixel-wise intensities over time and the max directional length of rain streaks or snowflakes are proposed. Based on the autocorrelation of each pixel's intensities over time, two temporal features are used for coarse classification of weather conditions according to their visual effects. On the other hand, features are extracted for fine classification of video clips with rain and snow. The classification results on 249 video clips associated with different weather conditions indicate the effectiveness of the extracted features, by using C-SVM as the classifier.

Keywords feature extraction, classification, rain, snow, illumination variation, weather condition, autocorrelation function

1 Introduction

Scene modeling is an important subject in many different applications of outdoor video analysis and computer vision, such as motion detection [1], object tracking [2], video surveillance [3], robot navigation [4], and video retrieval [5]. Previous research in this field has underestimated the importance of weather conditions for modeling, revealing that the applications mentioned above appear poor results when weather condition becomes to change. In other words, a certain model only works under some circumstance. A typical model adaptive to moving passive objects, gradual illumination variation and camouflage is an appropriate case in point [6]. A uniform scene model associated with all weather conditions is over complicated. Hence, different scene models are in demand.

On the other hand, study concentrating on modeling and removing the visual effects of various weather conditions is in progress. In single image, haze is successfully removed [7–10]. Rain streaks and snowflakes are eliminated from video [11–14]. A transform from heavy rain in distant view to fog has been successfully employed by selecting camera parameters [15]. However, a general model on different weather conditions, which adapts not only to fog and haze but also to snow and rain, is still hard to be established.

Therefore, recognition of different weather conditions becomes a promising new topic. The existing methods are either model switching on scenes changing in brightness caused by varying weather conditions or some qualitative classification of weather conditions. In Ref. [16], outdoor scenes are composed of static pixels containing stationary objects and dynamic pixels associated with moving passive objects, even including gradual or sudden illumination variation. Meanwhile, weather conditions are classified into steady (fog, mist and haze) and dynamic (rain, snow and hail), considering their physical properties or the visual effects they produce [12].

The aim of the paper is to give quantitative criteria for classification of different weather conditions. In order to recognize different weather conditions, features extracted for classification of weather conditions according to the video clip they belong to are proposed. Considering the correlations of pixel-wise intensities over time, we firstly classify weather conditions into steady (fog and gradual illumination variation caused by time of day [17]), dynamic (rain and snow), and nonstationary (fast illumination variation caused by fast motion of clouds in clear weather). Then, we employ four direction templates to analyze the max directional length of

Received January 29, 2011; accepted April 25, 2011

Xudong ZHAO (✉), Peng LIU, Jiafeng LIU, Xianglong TANG
School of Computer Science, Harbin Institute of Technology, Harbin 150001, China
E-mail: percydd@163.com

motion blur caused by rain streaks or snowflakes, and hence rain streaks can be distinguished from snowflakes. We make an experiment by extracting features from 249 video clips associated with different weather conditions and classifying the video clips according to their weather conditions. The classification results indicate the effectiveness of the extracted features by using C-SVM as the classifier.

The rest of the paper is as follows. In Sect. 2, features derived from autocorrelations of pixel-wise intensities over time are extracted for coarse classification. In Sect. 3, some spatial feature derived from the directional lengths of motion blur is selected for fine classification. In Sect. 4, the experimental results are discussed. Conclusion is made in Sect. 5.

2 Feature extraction for coarse classification

As to coarse classification of different weather conditions, the main problem is to extract effective features which can preserve the similar weather conditions, while separate the different ones. Taken illumination variations into account, weather conditions can be experientially classified as steady, dynamic, and nonstationary in some broad way (see Fig. 1). Gradual illumination variation appears steady intensities. Fast illumination variation shows continuity in brightness change. As to rain or snow, there are two intensity states representing either the motion blur of snowflakes or rain streaks or the background.

Focused on each pixel, intensities of image sequences representing scenes with various weather conditions are just a set of time series. In time series preprocessing, autocorrelation function (ACF), which is regarded as an important statistical quantity, is as follows [18]:

$$\rho(k) = \frac{\gamma(k)}{\gamma(0)} = \frac{\mathrm{Cov}\,(X_{t+k}, X_k)}{\mathrm{Cov}\,(X_k, X_k)}, \quad k = 0, \pm 1, \pm 2, ..., \quad (1)$$

where t and k represent the current and interval frame number of time series $\{X_t, t \in T\}$, respectively. γ is the covariance function. Let X_t be the intensity value of frame t. Considering the limited time length T, we rewrite Eq. (1) as follows:

$$\hat{\rho}(k) \approx \frac{\sum_{t=1}^{T-k} \left(X_t - \bar{X}\right)\left(X_{t+k} - \bar{X}\right)}{\sum_{t=1}^{T} \left(X_t - \bar{X}\right)^2}, \quad (2)$$

where $\bar{X}$ represents the time-average value of $\{X_t\}$ when k is far less than T.

We achieve our broad classification by extracting two effective features representing different weather conditions, as shown in Fig. 2, and deriving from the corresponding ACF plots illustrated in Fig. 3. In Fig. 2, we select three video clips with very different weather conditions, each of which is at a length of 124 frames with its selected area 51×51 square. In Fig. 3, we show three line graphs corresponding to central pixels in selected areas of scenes in different weather conditions shown in Fig. 2. These line graphs are named as ACF plots, where the horizontal and vertical axis respectively represents the interval frame numbers and the ACF value calculated by Eq. (2). The blue, red and black color plots denote ACF plots, the corresponding quadratic fit, and the temporal average of ACF value.

As is shown in Fig. 3, video clips representing different weather conditions have different ACF plots. Obviously, intensity change at the pixel affected by fast illumination

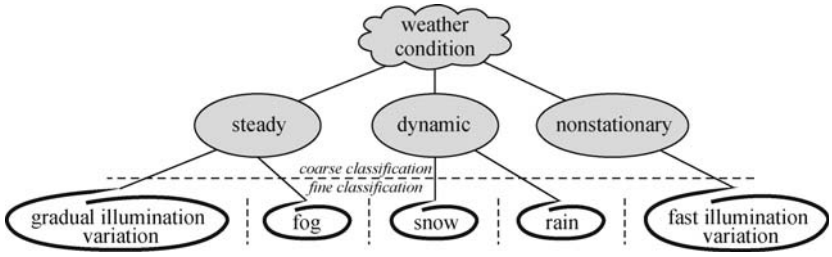

Fig. 1 Sketch map of classification scheme

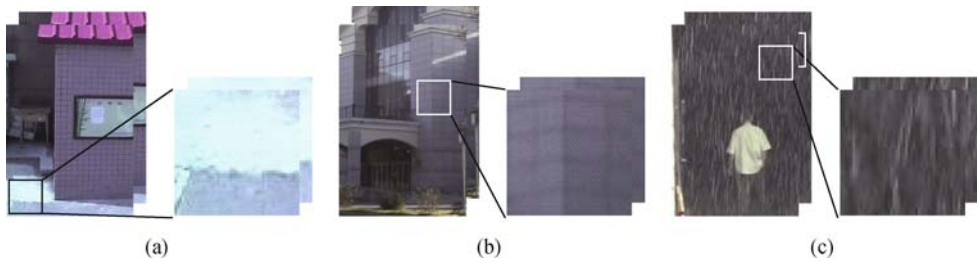

Fig. 2 Three video clips in different weather conditions. (a) Fast illumination variation; (b) gradual illumination variation; (c) rain

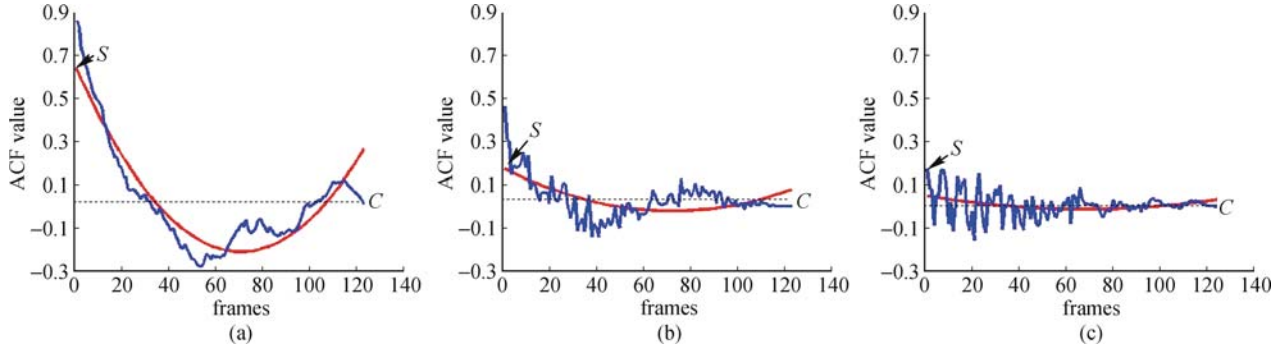

Fig. 3 ACF plots in different weather conditions. (a) Fast illumination variation; (b) gradual illumination variation; (c) rain

variation appears strong short-time autocorrelation (see Fig. 3(a)). On the other hand, rain streaks or snowflakes show two brightness states at a fixed pixel, which leads to weaker time-average ACF value than that of gradual illumination variation. In order to indicate this appearance, we make a comparison between the time-average ACF values of the corresponding pixels in two selected areas in Figs. 2(b) and 2(c), as is shown in Table 1.

Table 1 A comparison between time-average ACF values in selected areas of video clips with different weather conditions

	weather conditions	
	gradual illumination variations	rain
maximum mean of ACF value	0.1119	0.0044
minimum mean of ACF value	0.0315	0.0027
positive difference counts	2601	
ratio	100	

In Table 1, the maximum and minimum of time-average ACF values in two selected areas representing gradual illumination variation (see Fig. 2(b)) and rain (see Fig. 2(c)) are calculated. Moreover, we counts the temporal average ACF positive differences of the corresponding locations between the two selected areas, and obtain a ratio of the positive counts to all pixels in selected area.

Therefore, two effective temporal features are extracted to separate these different weather conditions, as are represented as follows:

$$\begin{cases} S = \underset{y\in\Omega}{\text{mean}}(\hat{f}_y(0)), \\ C = \underset{y\in\Omega}{\text{mean}}\left(\sum_{k=1}^{T-1}\dfrac{\hat{\rho}_y(k)}{T}\right), \end{cases} \tag{3}$$

where $\hat{\rho}_y(k)$ is equivalent to ACF value at location y in interval frame number k, as is expressed in Eq. (2). Ω is the selected area. $\hat{f}(k)$ represents the quadratic fit of $\hat{\rho}(k)$. Feature S indicates whether the spatial average of the selected area of a video clip in weather condition under classification is only in short-time autocorrelation of intensity change or not. Feature C represents whether the spatial average of selected area of the video clip has weaker time-average autocorrelation of intensity change or not. We choose patterns calculated by Eq. (3) at pixels in selected areas shown in Fig. 2, and train a linear classifier pairwise, based on minimum squared-error procedures. Obviously, patterns are easily classified, as is shown in Fig. 4. The red, green and blue patterns represent nonstationary, steady and dynamic weather conditions (see Fig. 4). Thus, the extracted features in Eq. (3) effectively classify weather conditions into steady, dynamic and nonstationary, as is shown in Fig. 1.

3 Feature extraction for fine classification

We can easily recognize gradual illumination variation

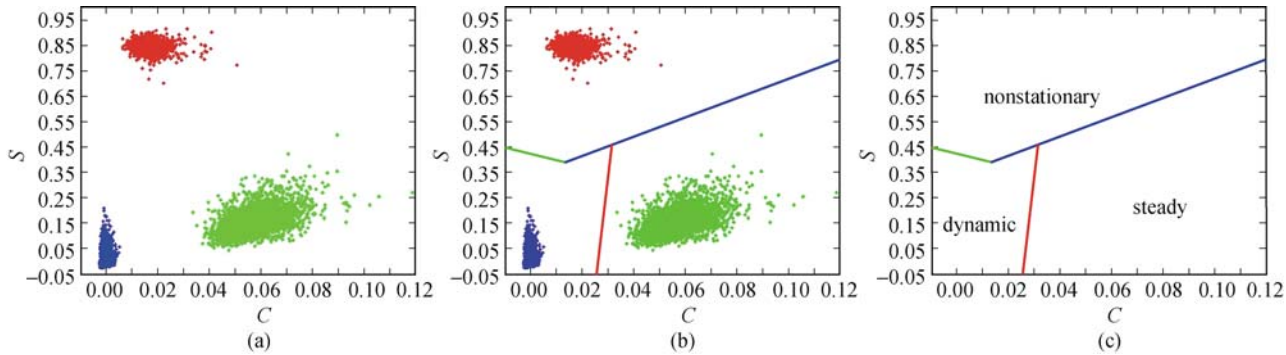

Fig. 4 Classifier design on patterns derived from Fig. 2 in different weather conditions. (a) Patterns separate after extraction of effective features. Here the red, green and blue patterns respectively represent nonstationary, steady and dynamic weather conditions; (b) linear classification based on minimum squared-error procedures; (c) a coarse classifier which generally classifies new patterns into nonstationary, steady and dynamic weather conditions

from fog by using the method mentioned in Ref. [10]. Therefore, we only discuss feature for fine classification of rain and snow in this section. Rain streaks and snowflakes are quite different in directional lengths of their motion blurs, taken the exposure time of camera into account. Thus, we firstly detect the locations of their motion blurs, and then extract the spatial feature for fine classification between dynamic weather conditions.

3.1 Motion blur detection for feature extraction

First, rain streaks or snowflakes are to be detected from static pixels of background. Two states, which represent the static background and the motion blur respectively, appear over time. Thus, the K-means clustering algorithm for detection of motion blur is taken into account. Let K be 2. At each pixel, two cluster centers ω_{b} and ω_{c}, which represent the static background and the motion blur, are initialized to be the minimum and maximum of the intensity value over time. Euclidean distance d representing the distance between the current intensity value I at pixel p and the cluster center ω is computed as follows:

$$d\left(I_p, \omega\right) = \left|I_p - \omega\right|. \tag{4}$$

Thus, I at p is divided into the motion blur cluster, if $d\left(I_p, \omega_{\mathrm{c}}\right)$ is smaller than $d\left(I_p, \omega_{\mathrm{b}}\right)$, or vice versa. After that, the center of cluster K is updated as follows:

$$\omega(n+1) = \frac{1}{|C(n)|} \sum_{I_p \in C(n)} I_p. \tag{5}$$

K-means clustering continues until the cluster centers converge. The respective detection results of rain and snow are shown in Fig. 5. Considering the limitation of frame length of video, the detection results appear a little mistake. Yet, it is allowed, because the identification speed demands more than correctness of detection. Moreover, the existent influence on fine classification is weaken, taken statistical results derived from a large amount of data into account.

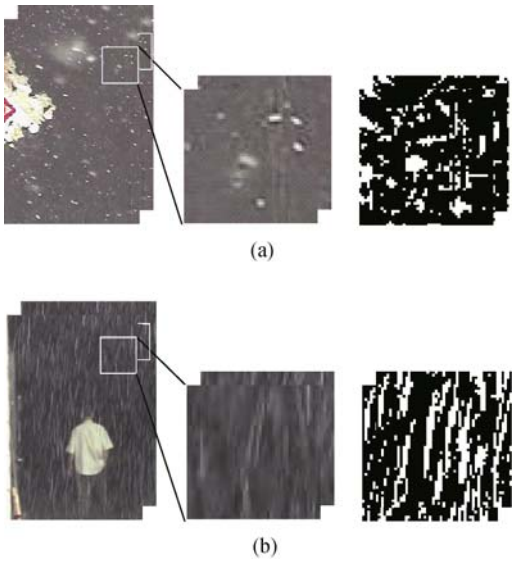

Fig. 5 Results of detection in two video clips with rain and snow. Each video is at a length of 124 frames with its selected area 51×51 square. (a) Snow; (b) rain, as is also shown in Fig. 2(c)

3.2 Feature extraction for fine classification

Differences between the results of rain and snow detection shown in Fig. 5 are apparent. Rain has obvious shapes of streak on vertical direction considering the exposure time of camera, when there is no wind; yet, snow appears as small flakes. However, it is hard to extract shape features in vertical direction right from the detection results in Fig. 5. Although better detection results can improve the effect of shape feature extraction, it is still annoying spending long time here, other than on latter applications such as tracking and recognition in bad weather.

Therefore, directional length, which approximates to the shape of motion blur, is recorded. Statistical counts on four directional lengths lead to successful classification of rain and snow. First, we establish four directional templates (see Fig. 6). Each template is 2×2 square, with a black point indicating the current unit under treatment. The four templates are expressed as T_{v}, T_{h}, $T_{d_{\mathrm{p}}}$, and $T_{d_{\mathrm{n}}}$, which represent the vertical, horizontal, principal and negative diagonal direction, respectively.

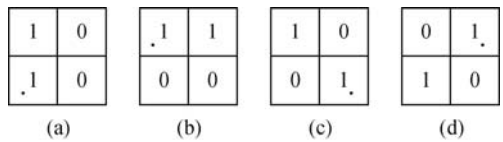

Fig. 6 Four directional templates. (a) T_{v} for vertical length calculation; (b) T_{h} for horizontal length calculation; (c) $T_{d_{\mathrm{p}}}$ for principal diagonal length calculation; (d) $T_{d_{\mathrm{n}}}$ for negative diagonal length calculation

On the other hand, frames of the detection results are represented as a logical matrix named as *Logic*, where the element with corresponding pixel covered with motion blur equals 1. When a directional template moves on a frame of the *Logic*, the length of motion blur in this direction will be calculated in a workspace named as *Frame_work* of this direction. The procedure is illustrated in Fig. 7.

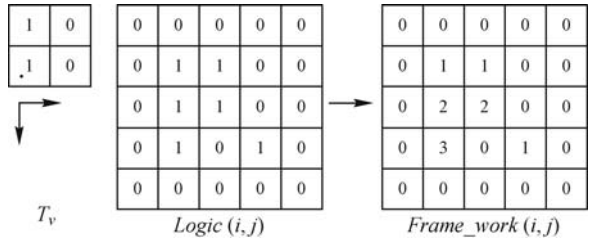

Fig. 7 A procedure of recording length of motion blur in vertical direction

Meanwhile, the temporary counts of length are stored in a workspace named as *Histogram* by adding one to the bar of the same index number as corresponding length. When all the frames of the detection results have been processed, four histograms recording all lengths of the directions over time are obtained. Figure 8 illustrates the vertical histogram. As can be easily seen in Fig. 8, the histogram on vertical length of snow holds lower average of vertical length than that of rain. In fact, histograms of different directions have different weighted averages, as have a uniform expression:

$$W = \frac{\sum_{i=1}^{L} Histogram(i) \cdot i}{\sum_{i=1}^{L} Histogram(i)}. \tag{6}$$

Equation (6) represents weighted average of lengths in four different directions, which is described as one form of W_{v}, W_{h}, $W_{d_{\mathrm{p}}}$, and $W_{d_{\mathrm{n}}}$ in the corresponding direction. Thus, weighted average of the max directional length is regarded as an effective feature for fine classification of rain and snow, as is expressed as follows:

$$W = \max(W_{\mathrm{v}}, W_{\mathrm{h}}, W_{d_{\mathrm{p}}}, W_{d_{\mathrm{n}}}). \tag{7}$$

In order to indicate the effectiveness of feature W, we select six video clips with different rain and snow (see Fig. 9). Each is at a length of 124 frames with its selected area 51×51 square. Moreover, we compare the feature values of W, together with two video clips shown in Fig. 5, as is shown in Table 2. Therefore, a feature vector $(S, C, W)^{\mathrm{T}}$ is obtained, taken features mentioned in Eqs. (3) and (7) into account meanwhile.

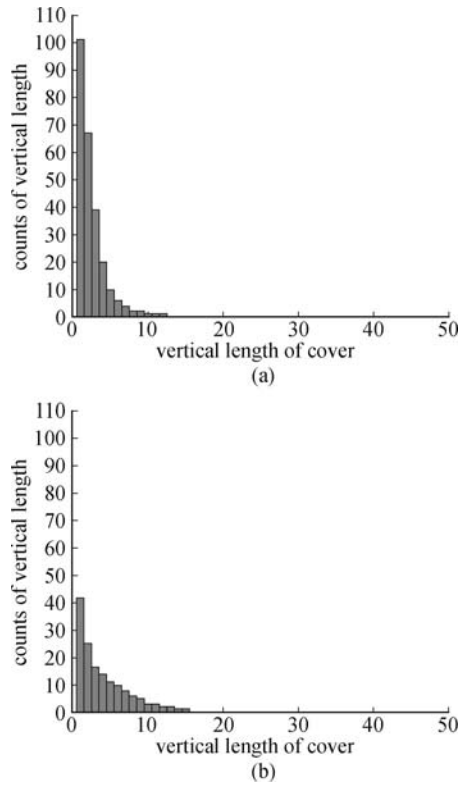

Fig. 8 Two histograms recording vertical length of snow and rain. (a) Histogram of snow; (b) histogram of rain (The two histograms are associated with scenes shown in Fig. 5. As a matter of convenience, counts of the vertical length divided by the length of frame are shown instead.)

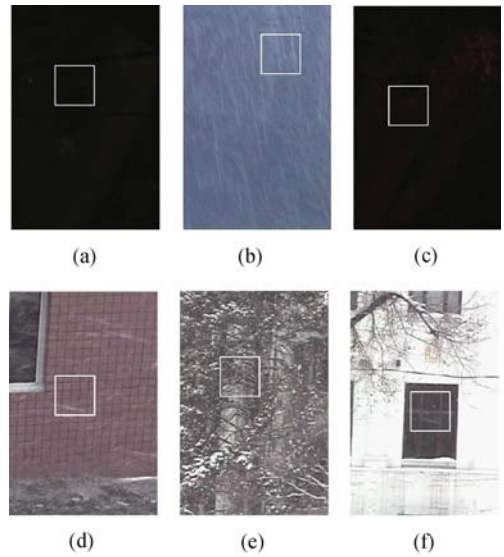

Fig. 9 Six video clips in rain or snow. (a) Sleet at night; (b) light rain; (c) snow at night; (d) snow at a long exposure time; (e) heavy snow; (f) light snow

Table 2 Spatial feature values extracted from videos with different states of rain or snow

label in figures	rain or snow	W_{v} value
Figure 5(a)	heavy snow	2.4134
Figure 5(b)	heavy rain	4.0333
Figure 9(a)	sleet at night	2.1763
Figure 9(b)	light rain	4.0333
Figure 9(c)	snow at night	2.1958
Figure 9(d)	snow at long exposure time	2.2623
Figure 9(e)	heavy snow	2.1133
Figure 9(f)	light snow	2.0372

4 Experimental results and discussion

We have found no other researches on weather classification. Thus, we select 249 video clips deriving from captured videos, film clips, existing public video data set and webcams with different weather conditions mentioned in Fig. 1, as is shown in Fig. 10. Moreover, we choose a relatively uniform area in each video for classification. By using leave-one-out method, we repeat learning the C-SVM classifier following the step from coarse to fine classification as shown in Fig. 1 by using the obtained patterns as expressed in Eq. (3), Eq. (7) and in Ref. [10]. The experimental results shown in Table 3 indicate the robustness of our extracted features, for the percent of accuracy on classification of weather

Fig. 10 A photomontage of 249 video clips (Red line departs different groups of video clips with visual effects of different weather conditions. The green frames show the classification error. These videos are selected from data set — SCOTIA, which can be downloaded from http://pr-ai.hit.edu.cn/scotia/.)

Table 3 Classification results of 249 selected videos

weather conditions	right/s	wrong/s
gradual illumination variation	45	5
fog	50	0
snow	42	8
rain	44	6
fast illumination variation	49	0

conditions is 92.37%.

Yet, there are 19 errors. Gradual illumination variation is misclassified into fog, because we select areas on sky or on ground covered with snow. Moreover, rain and snow are inter-misclassified for unfixed exposure time.

5 Conclusion

We extract effective features for quantitative classification method on visual effects of different weather conditions. Two temporal features derived from autocorrelations of pixel-wise intensity values over time are extracted for coarse classification. Moreover, a feature representing the max directional length of rain streaks or snowflakes is proposed. We make experiments on 249 video clips in gradual illumination variation, fog, snow, rain, and fast illumination variation, and demonstrate the effectiveness of our extracted features.

Acknowledgements This work was supported by the National Natural Science Foundation of China (Grant No. 60702032), the Natural Scientific Research Innovation Foundation in Harbin Institute of Technology (No. HIT.NSRIF.2008.63), and China Academy of Space Technology Innovation Foundation (No. CAST200814).

References

1. Zhang B C, Gao Y S, Zhao S Q, Zhong B. Kernel similarity modeling of texture pattern flow for motion detection in complex background. IEEE Transactions on Circuits and Systems for Video Technology, 2011, 21(1): 29–38
2. Khan Z H, Gu I Y H, Backhouse A G. Robust visual object tracking using multi-mode anisotropic mean shift and particle filters. IEEE Transactions on Circuits and Systems for Video Technology, 2011, 21(1): 74–87
3. Woo H, Jung Y M, Kim J G, Seo J K. Environmentally robust motion detection for video surveillance. IEEE Transactions on Image Processing, 2010, 19(11): 2838–2848
4. Gouko M, Ito K. An action generation model by using time series prediction and its application to robot navigation. International Journal of Neural Systems, 2009, 19(2): 105–113
5. Geetha M K, Palanivel S. A novel event-oriented segment-of-interest discovery method for surveillance video. International Journal of Computational Intelligence Systems, 2009, 2(1): 39–50
6. Maddalena L, Petrosino A. Video classification and shot detection for video retrieval applications. IEEE Transactions on Image Processing, 2008, 17(7): 1168–1177
7. Narasimhan S G, Nayar S K. Vision and the atmosphere. International Journal of Computer Vision, 2002, 48(3): 233–254
8. Narasimhan S G, Nayar S K. Contrast restoration of weather degraded images. IEEE Transactions on Pattern Analysis and Machine Intelligence, 2003, 25(6): 713–724
9. Fattal R. Single image dehazing. In: Proceedings of International Conference on Computer Graphics and Interactive Techniques. 2008, 1–9
10. He K, Sun J, Tang X. Single image haze removal using dark channel prior. In: Proceedings of IEEE Conference on Computer Vision and Pattern Recognition. 2009, 1956–1963
11. Garg K, Nayar S K. Detection and removal of rain from videos. In: Proceedings of IEEE Conference on Computer Vision and Pattern Recognition. 2004, 528–535
12. Garg K, Nayar S K. Vision and rain. International Journal of Computer Vision, 2007, 75(1): 3–27
13. Zhang X, Li H, Qi Y, Leow W, Ng T. Rain removal in video by combining temporal and chromatic properties. In: Proceedings of the International Conference on Multimedia and Expo. 2006, 461–464
14. Barnum P, Kanade T, Narasimhan S G. Spatio-temporal frequency analysis for removing rain and snow from videos. In: Workshop on Photometric Analysis for Computer Vision. 2007
15. Garg K, Nayar S K. When does a camera see rain? In: Proceedings of the Tenth IEEE International Conference on Computer Vision. 2005, 2: 1067–1074
16. Li L, Huang W, Gu I Y, Tian Q. Statistical modeling of complex backgrounds for foreground object detection. IEEE Transactions on Image Processing, 2004, 13(11): 1459–1472
17. Toyama K, Krumm J, Brumitt B, Meyers B. Wallflower: principles and practice of background maintenance. In: Proceedings of IEEE Conference on Computer Vision and Pattern Recognition. 1999, 256–261
18. Fan J Q, Yao Q W. Nonlinear Time Series: Nonparametric and Parametric Methods. New York: Springer-Verlag, 2008

Xudong ZHAO was born in 1980. He received his master degree from the Harbin Institute of Technology, Harbin, China, in 2005. He is a Ph.D candidate in computing science of the Harbin Institute of Technology. His current research interests include image processing and computer vision.

Peng LIU was born in 1973. He received his master degree and Ph.D degree from the Harbin Institute of Technology, Harbin, China, in 2003 and 2007, respectively. He is currently an instructor at the Harbin Institute of Technology, and member of

China Computer Federation. His current research interests include pattern recognition, image processing and computer vision.

Jiafeng LIU was born in 1968. He received his Ph.D degree from the Harbin Institute of Technology, Harbin, China, in 1996. He is currently an associate professor at the Harbin Institute of Technology, and a senior member of China Computer Federation. His current research interests include pattern recognition, image processing and computer vision.

Xianglong TANG was born in 1960. He received his master degree and Ph.D degree from the Harbin Institute of Technology, Harbin, China, in 1986 and 1995, respectively. He is currently professor at the Harbin Institute of Technology. He is also a senior member of China Computer Federation. His main research interests include OCR, biometrics, image processing, pattern recognition theory, etc.